Isam Eddine Lamri, Sarosh Ahmad*, Mohammed Farouk Nakmouche, Adnan Ghaffar, Diaa E. Fawzy, A.M.M.A. Allam, Esraa Mousa Ali, Mariana Dalarsson and Mohammad Alibakhshikenari*

Design and development of a graphene-based reconfigurable patch antenna array for THz applications

https://doi.org/10.1515/freq-2022-0051
Received March 4, 2022; accepted June 21, 2022;
published online July 11, 2022

Abstract: This paper presents a graphene-based antenna array for terahertz (THz) applications. The suggested antenna array has four radiating square shaped patches fed by a coplanar waveguide (CPW) technique. The proposed antenna array operates at the three frequencies with operational bandwidths of 1.173–1.210 THz (at 1.19 THz), 1.270–1.320 THz (at 1.3 GHz), and 1.368–1.346 THz (at 1.4 GHz). The total area of the antenna array is reported as $1000 \times 1000\ \mu m^2$, printed on a Silicon substrate with a thickness of 20 μm and a dielectric constant of $\epsilon_r = 11.9$. To enhance the structure's performance and optimize the feeding network, a parametric analysis was performed using the FDTD technique. Furthermore, the key properties of the proposed antenna array, such as resonance frequency, peak gain, and radiation efficiency, may be changed by adjusting the chemical potentials of the graphene in the antenna array. The use of graphene's chemical potential tuneability yields exceptional results comparing to the recent research outputs, with a peak gain and radiation efficiency of 10.45 dB and 70%, respectively. These results show the performance of the suggested design for constructing antenna arrays for use in THz applications.

Keywords: antenna array; graphene-based reconfigurable antenna; terahertz wireless applications; triple-band.

***Corresponding authors: Sarosh Ahmad**, Department of Systems and Computer Engineering, Carleton University, Ottawa, ON, K1S 2P3, Canada; and Department of Signal Theory and Communications, Universidad Carlos III de Madrid, 28911 Leganés, Madrid, Spain, E-mail: saroshahmad@sce.carleton.ca; and **Mohammad Alibakhshikenari**, Department of Signal Theory and Communications, Universidad Carlos III de Madrid, 28911 Leganés, Madrid, Spain, E-mail: mohammad.alibakhshikenari@uc3m.es
Isam Eddine Lamri, Electronic Research Laboratory of Skikda (LRES), University of Skikda, Skikda, Algeria, E-mail: isam.lamri@univ-skikda.dz
Mohammed Farouk Nakmouche and Diaa E. Fawzy, Faculty of Engineering, İzmir University of Economics, Izmir, Turkey, E-mail: nakmouche.MFarouk@gmail.com (M.F. Nakmouche), diaa.fawzy@gmail.com (D.E. Fawzy)
Adnan Ghaffar, Department of Electrical and Electronic Engineering Auckland University of Technology, Auckland, New Zealand, E-mail: aghaffar@aut.ac.nz
A.M.M.A. Allam, Department of Communication Engineering, German University in Cairo, Cairo, Egypt, E-mail: abdelmegid.allam@guc.edu.eg
Esraa Mousa Ali, Faculty of Aviation Sciences, Amman Arab University, Amman 11953, Jordan, E-mail: esraa_ali@aau.edu.jo
Mariana Dalarsson, School of Electrical Engineering and Computer Science, KTH Royal Institute of Technology, SE 100-44 Stockholm, Sweden, E-mail: mardal@kth.se

1 Introduction

In recent years, antennas in the THz frequency ranges from 0.1 to 10 THz have been studied and developed for different applications. The development of tiny devices capable of transmitting and receiving data at low power with the highest possible data rates and ultra-wide bandwidth is required by new applications in the field of terahertz communication systems [1]. As a result, shifting carrier frequencies to the terahertz band is a realistic alternative for meeting the long-term needs of the next generation of wireless communication systems [2]. However, as compared to lower band systems, the terahertz band has specific characteristics, including higher transmission path loss and additional molecular losses owing to absorption [3]. Many researches have been conducted to address these issues, highly directional antennas being recommended as a way to overcome losses and to increase the link capacity. On the other hand, existing radio frequencies (RF) and optical transceivers, have many drawbacks, such as their size, design complexity, and energy consumption. These constraints have prompted researchers to investigate novel nanomaterials as the foundation for next-generation electronics beyond silicon. Graphene is one of the most promising alternatives [4].

Graphene exhibits good electrical conductivity, electrical conductance controllability, and plasmon properties,

if integrated in antennas, it shows better radiation properties than typical counterparts metal antennas. This is due to its good conductivity and to the fact that its chemical potential may be altered by applying bias voltage to its surface conductivity, which in turns alters the value of graphene's surface impedance [5]. It is anticipated that such a device might attain rates of up to terabits per second. To function at nanoscales, traditional antennas would need to operate at very high frequencies, making it an impractical choice. However, graphene's distinctive slower electron mobility allows it to work at higher frequencies, making it a viable candidate for a Nano-sized antennas [6, 7]. As a consequence, graphene-based materials offer some potential in the development of reconfigurable antennas. Exploiting the electrical characteristics of graphene material, a variety of adjustable graphene antennas have been developed for various purposes in the THz frequency region [7–21]. In 2012, the first research on graphene in a microwave antenna was reported [6]. The obtained results supported the theoretical models and confirmed that a graphene-based Nano-patch antenna with dimensions of a few micrometers resonates in the terahertz region. Furthermore, the antenna resonance frequencies were found to be dependent on the dimensions of both the graphene patch and the dielectric substrate constant. The radiation pattern was found to be extremely comparable to that of an analogous metallic antenna [7]. Describes the design and numerical analysis of a reconfigurable graphene antenna. The author developed a two and a four-beam reconfigurable Yagi-Uda antenna with graphene switches. In [9], Seyed Arash Naghdehforushha and Gholamreza Moradi propose THz graphene-based patch array antennas. The structure is based on two rectangular patch elements in which surface plasmon wave (SPP) behavior is presented. In [10], a dual-band graphene antenna array with parasitic-coupled feed, placed on a Photonic-Band-Gap (PBG) dielectric substrate, and operating in the frequency band from 0.85 to 1.04 THz is presented.

Graphene is a fascinating material that has gained a lot of attention recently, especially after Andre Geim and Konstantin Novoselov, who originally isolated Graphene in 2004, were awarded the Nobel Prize in Physics in 2010. Graphene is a one-atom-thick film of hexagonally organized carbon atoms. With a thickness of one atom, it is the world's thinnest material. Furthermore, graphene is an excellent conductor of heat and electricity, as well as having remarkable light absorption properties. Graphene has a special structure that allows electrons to flow with minimum resistance. This allows electricity to move considerably faster than it would through metal, which is utilized in existing antennas. Moreover, when the electrons oscillate, they generate an electromagnetic wave known as the surface plasmon polariton wave above the graphene sheet. This would allow the antenna to function at the lower end of the terahertz frequency band, making it more efficient than conventional copper-based antennas.

The length and width of graphene-based Nano-patch antennas are expected to be in the micrometer range [22]. We would then ignore edge effects in this analysis and apply the electrical conductivity model established for infinite graphene sheets, as it has been experimentally proved that edge effects on graphene conductivity only arise in structures with dimensions much smaller than 100 nm [23]. The graphene's conductivity, shown in Figure 1, may be described by the Kubo formula [24], where the total conductivity is the addition of two distinct components, i.e.:

$$\sigma_{\text{total}} = \sigma_{\text{inter}} + \sigma_{\text{intra}} \tag{1}$$

The interband contribution:

$$\sigma_{\text{inter}} \simeq \frac{-je^2}{4\pi\hbar}\ln\left(\frac{2|\mu_c| - (\omega - j\Gamma)\hbar}{2|\mu_c| + (\omega - j\Gamma)\hbar}\right) \tag{2}$$

The intraband contribution:

$$\sigma_{\text{intra}} = \frac{-je^2K_BT}{\pi\hbar^2(\omega - j2\Gamma)} \times \left(\frac{\mu_c}{K_BT} + 2\ln\left(e^{-\frac{\mu_c}{K_BT}} + 1\right)\right) \tag{3}$$

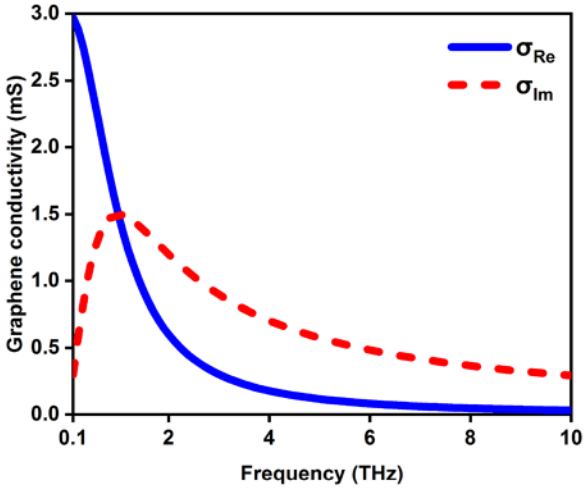

Figure 1: Conductivity of graphene for $\mu_c = 0.16$ eV, $\tau = 1$ ps and $T = 300$ K.

where:

T: temperature
K_B: Boltzmann constant
$\hbar$: reduced Plank's constant
μ_c: chemical potential
e: electron charge
Γ: scattering rate

At lower THz frequencies, intraband conductivity dominates whereas interband conductivity is insignificant [25]. Therefore, σ_{total} is due solely to the intraband contribution described by Eq. (3). This equation clearly shows that graphene's intraband conductivity is significantly reliant on μ_c and τ. Because the relaxation time ($\tau = 1/\Gamma$) is determined by the graphene sample quality [26], the value $\tau = 1$ ps was chosen as an optimal value to sustain the conductivity for the best performance of the graphene patch antenna [25], μ_c is determined from the density of charge carriers. We can only alter μ_c after production by using external DC bias. As a consequence, μ_c may be dynamically adjusted and the graphene-based antenna becomes frequency reconfigurable by altering DC voltage, which must be properly picked. Figure 2(a) and (b) reveal the values of the intra-band conductivity real and imaginary parts.

In this paper, a compact graphene-based antenna array of 1000 × 1000 μm^2 size is proposed for THz applications. The structure, mounted on Silicon substrate with relative permittivity $\varepsilon_r = 11.9$ and tan $\delta = 0.00025$, is fed by a 50 Ω CPW-based microstrip line. The paper is organized as follows. In Section 2, we provide the background information of graphene material properties. In Section 3, we presented the design of the graphene-based antenna array design. The simulation results; including S-parameters, radiation patterns, gain, radiation efficiency, and the graphene tunability are discussed in Section 4. Finally, the conclusions are given in Section 5.

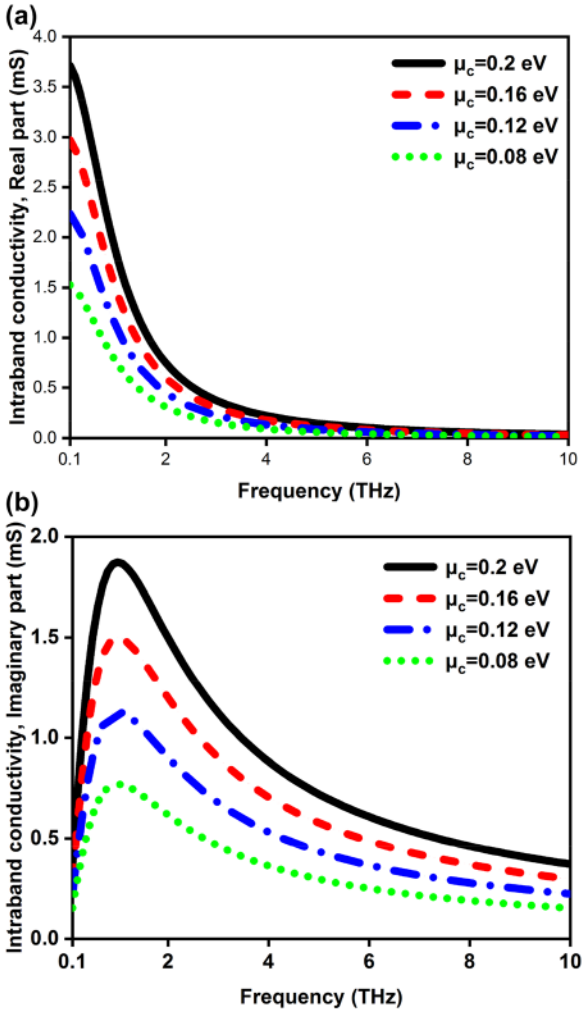

Figure 2: The intraband conductivity of graphene for $\tau = 1$ ps, $T = 300$ K and different μ_c values, (a) real part and (b) imaginary part.

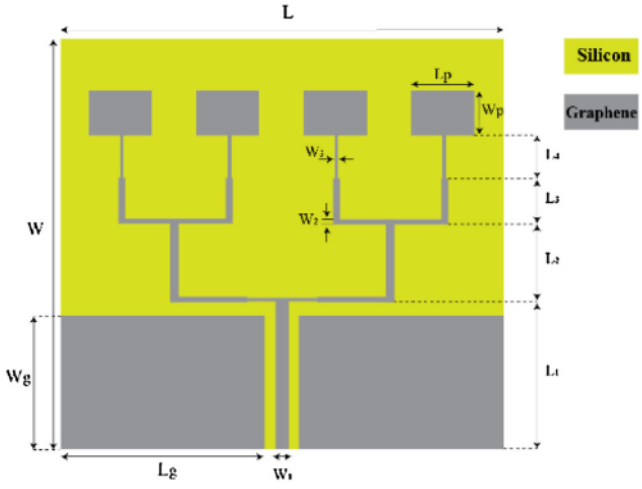

Figure 3: The proposed graphene antenna array design.

2 Design of a graphene-based patch antenna array

As illustrated in Figure 3, this study proposes a tri-band graphene-based coplanar waveguide (CPW) antenna array design for THz applications with a total substrate size of 1000 × 1000 × 20 μm^3. The substrate material is Silicon with a relative permittivity of $\varepsilon_r = 11.9$ and loss tangent of tan $\delta = 0.00025$. The antenna array is designed and simulated

in the CST microwave studio suite. In order to get a high antenna gain, the feeding network and the number of individual antenna element used are critical. A multi-element antenna array can achieve greater gain than a single element, and an optimized feeding network can enhance the gain. In general, the larger the number of individual antenna elements used, the higher the gain. The amplitude and phase of the current delivered to each antenna element are governed by a feeding network constructed using transmission line theories. To achieve 50–Ω, 70-Ω, and 100-Ω antenna array input impedance at the specified frequency bands, the feed line parameters (width and length) are necessary. The parameters are determined in order to match the feed to the resonant antenna element. The optimized feeding network and radiating patches with their dimensions are tabulated in Table 1.

3 Results and discussions

In this section, the designed antenna is analyzed and discussed. Figure 4 shows the reflection coefficient versus frequency of the proposed antenna array. The figure clearly shows that the antenna provides three operating bands: 1.173–1.210 THz, 1.270–1.320 THz, and 1.368–1.346 THz, for which S11 ≤ –10 dB and resonant frequencies at 1.19 THz, 1.297 THz, and 1.397 THz. The graphene material provides an excellent antenna performance due its high conductivity which leads to better antenna reflection. A maximum gain and a maximum efficiency of 9.43 dB is achieved at 1.27 THz, as shown in Figure 5, this high gain value is obtained by utilizing antenna arrays. The gain of the proposed array antenna will increase as the number of antenna array elements increases, but this will not be endlessly due to medium and surface wave losses. Comparing to the same design based on copper instead of graphene, only two bands were obtained with lower gain.

Table 1: The optimized dimensions of the proposed graphene antenna array.

Parameter	Value (μm)	Parameter	Value (μm)	Parameter	Value (μm)
L	1000	L_g	482	L_3	128
W	1000	W_g	296	L_4	82
L_p	95	L_1	302.5	W_1	16
W_p	145	L_2	200	W_2	12
				W_3	4

3.1 Surface current densities

To get better insight into the radiation mechanism of this antenna, the surface current densities of the proposed antenna array at the resonance frequencies are illustrated in Figure 6. It is observed from the graphs that the current is intense at the patch edges, feeding network edges, and at the central area of the ground, towards the direction of y-plane, which becomes more intense for a higher frequency. Besides, different current distributions are found for each resonant frequency which indicates the existence of different equivalent electrical paths forcing the patch to resonate at different frequencies.

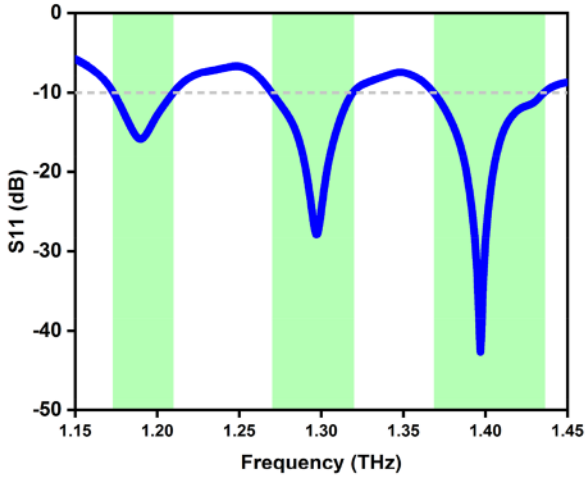

Figure 4: S11 of the proposed graphene antenna array.

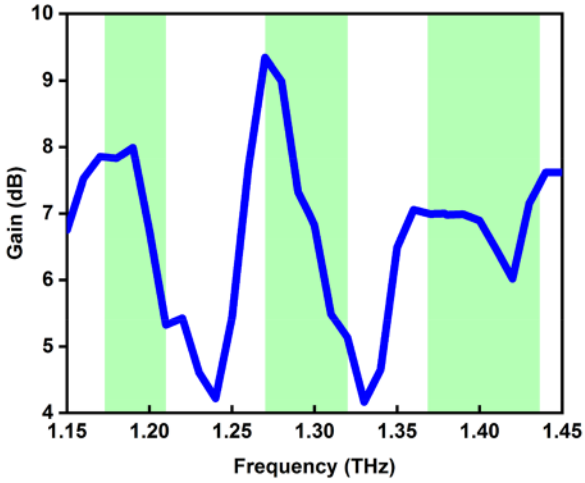

Figure 5: Gain of the proposed graphene antenna array.

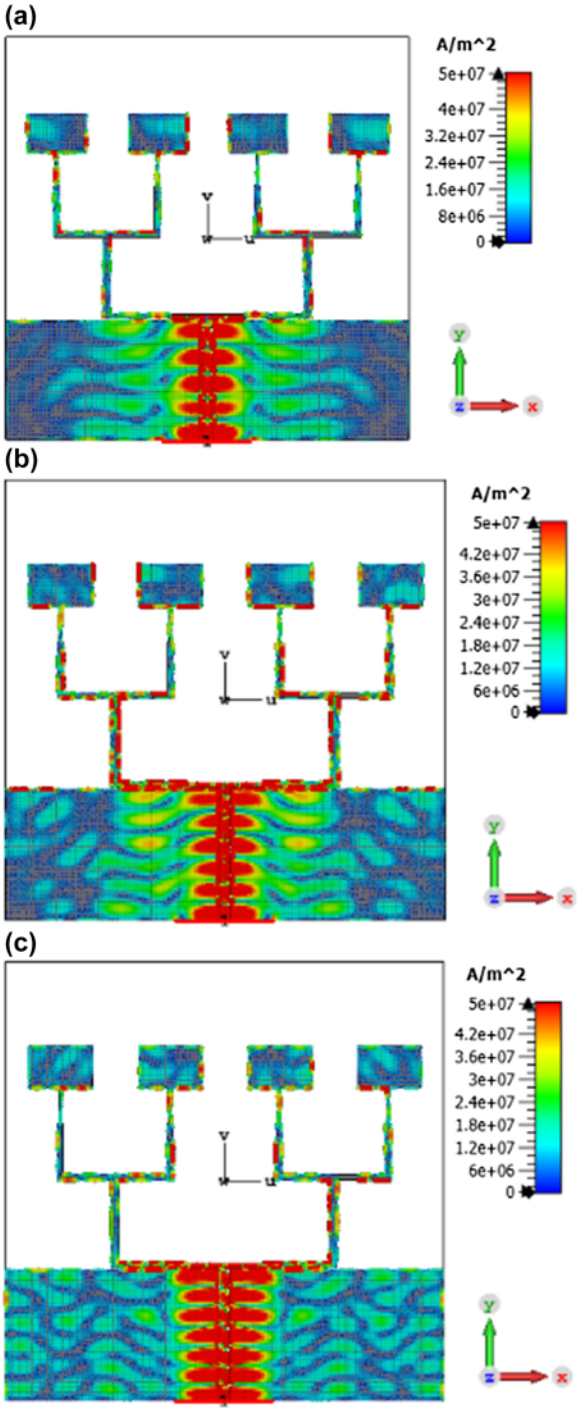

Figure 6: Surface current densities of the proposed graphene antenna array at resonant frequencies: (a) 1.19 THz, (b) 1.297 THz and (c) 1.379 THz.

3.2 Equivalent circuit model

A circuit model for the tri-band four elements antenna array fed by the coplanar waveguide (CPW) technique is developed. Using the advanced design system (ADS) software. The circuit model consists of nine inductors, seven capacitors, six resistors, and four resistor-inductor-capacitor (RLC) circuits connected in series with each other as shown in Figure 7(a). The RLC amounts are listed in Table 2. By varying the values of the resistors, the return loss of the circuit model can be varied while by changing the values of the capacitors and inductors, the S11 of the antenna can be tuned. The reflection coefficient of the circuit model is illustrated in Figure 7(b). It covers the bandwidth from 1.16 THz to 1.22 THz (about 60 GHz) centered at 1.19 THz, from 1.268 THz to 1.32 THz (about 52 GHz) centered at 1.297 THz, and from 1.355 THz to 1.365 THz (about 10 GHz) centered at 1.398 THz.

3.3 Radiation patterns

Figure 8 shows the radiation pattern of the antenna at resonant frequencies in E- and H-planes. It was observed that the radiation patterns of the graphene-based antenna array are nearly bidirectional at the lowest resonant frequency. However, at higher resonant frequencies, the radiation patterns tend to be broadside. The far-field polar plots of the E-plane show that the main lobe directions are 196°, 180°, and 185°. The achieved angular widths are 73.9°, 8.3°, 36.7° and the side lobe levels (SLL) are −7.5 dB, −1.8 dB, −3.8 dB for 1.19 THz, 1.297 THz and 1.379 THz, respectively. The high dielectric constant of the silicon substrate causes the most of the radiation to be directed towards the substrate. This is a frequent issue with antennas designed on high dielectric constant substrates.

An antenna design goal can be to maximize the Co-pol and decrease the cross-pol component in order to use different polarizations for transmitting/receiving. From Figure 9, it is clear that for all resonant frequencies, this goal is achieved which guarantees the use of different polarizations in the transmitting and receiving modes.

3.4 The effect of varying chemical potential μ_c

The chemical potential of the graphene patch, or the level in the distribution of electron energies where a quantum state is fairly probable to be populated or vacant, is another important statistic for evaluating the graphenne's performance. As shown in Eq. (3), the conductivity of graphene

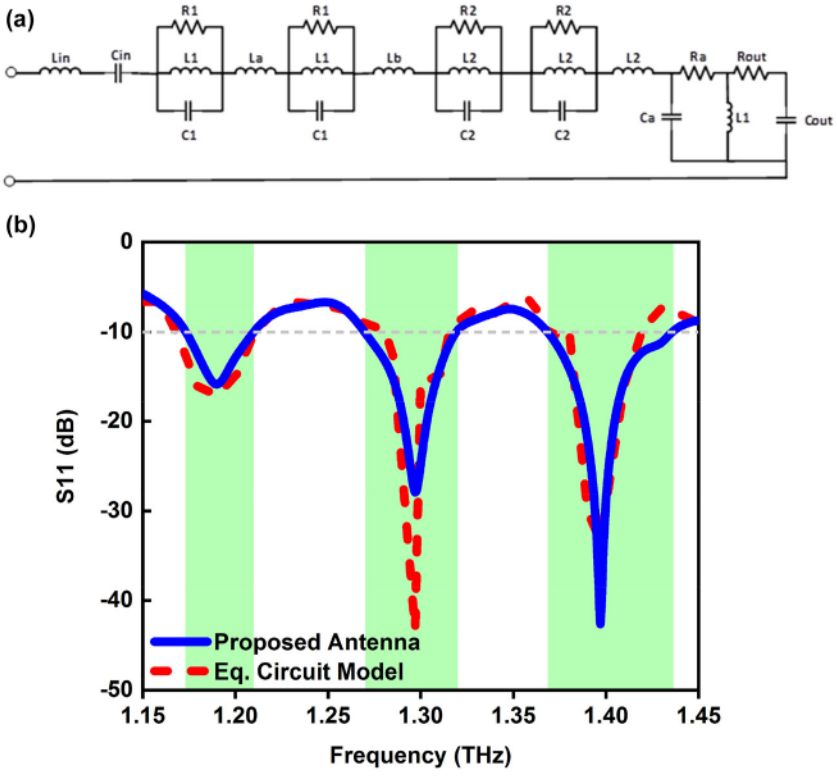

Figure 7: (a) Equivalent circuit model, (b) S11 obtained from circuit model.

Table 2: Lumped element components values of the equivalent circuit model.

Capacitors	Values (fF)	Inductors	Values (pH)	Resistors	Values (Ω)
C_{in}	1.8	L_{in}	1	$R1$	300
C_1	20	L_1	0.2	$R2$	100
C_2	10	L_2	1	R_a	25
C_a	0.1	L_a	4	R_{out}	0.01
C_{out}	95	L_b	2		

can be adjusted by applied external electric field through DC bias, which modifies the charge density [24]. Eq. (4) shows the relation the chemical potential μ_c and the applied bias [24].

$$\frac{2\epsilon_b E_b}{e} = \frac{2}{\pi\hbar^2 v_F^2}\int_0^\infty \epsilon(f_d(\epsilon) - f_d(\epsilon + 2\mu_c))d\epsilon \tag{4}$$

The variation of the μ_c with the applied DC bias is shown in Figure 10. For different values of electrostatic bias, μ_c can be varied in the range [–1 eV; 1 eV]. The thinner the graphene layer, the less voltage range is required for the variation of μ_c between these ranges [27], and Smaller values of chemical potential result in a small absorption cross-section, which limits graphene's radiation efficiency, whereas greater values give larger absorption cross-section and lead to an enhancement of the radiation efficiency. In this work, μ_c is taken in the range from 0.0 to 0.12 eV, for which a so small and positive external DC voltage is needed.

Figure 11(a)–(c) depict the effect of variation of μ_c on the frequency responses, gain, and radiation efficiency of the proposed antenna array. The variation in the chemical potential of graphene material leads to shift the frequency response keeping the impedance bandwidth. The gain and efficiency of the standard reference exhibit an important improvement with increasing μ_c, compared to $\mu_c = 0$ eV, the array's gain and efficiency are enhanced on the average by about 1.3 dB and 10% for μ_c = 0.12 eV, respectively. The values of μ_c are kept smaller so that it can be achieved for a low value of the externally applied DC voltage. Table 3 presents a comparison of the array performance for different values of μ_c.

This results of varying chemical potential μ_c clearly show that bias helps controlling antenna array efficiency and gain but slightly modifies the resonant frequencies.

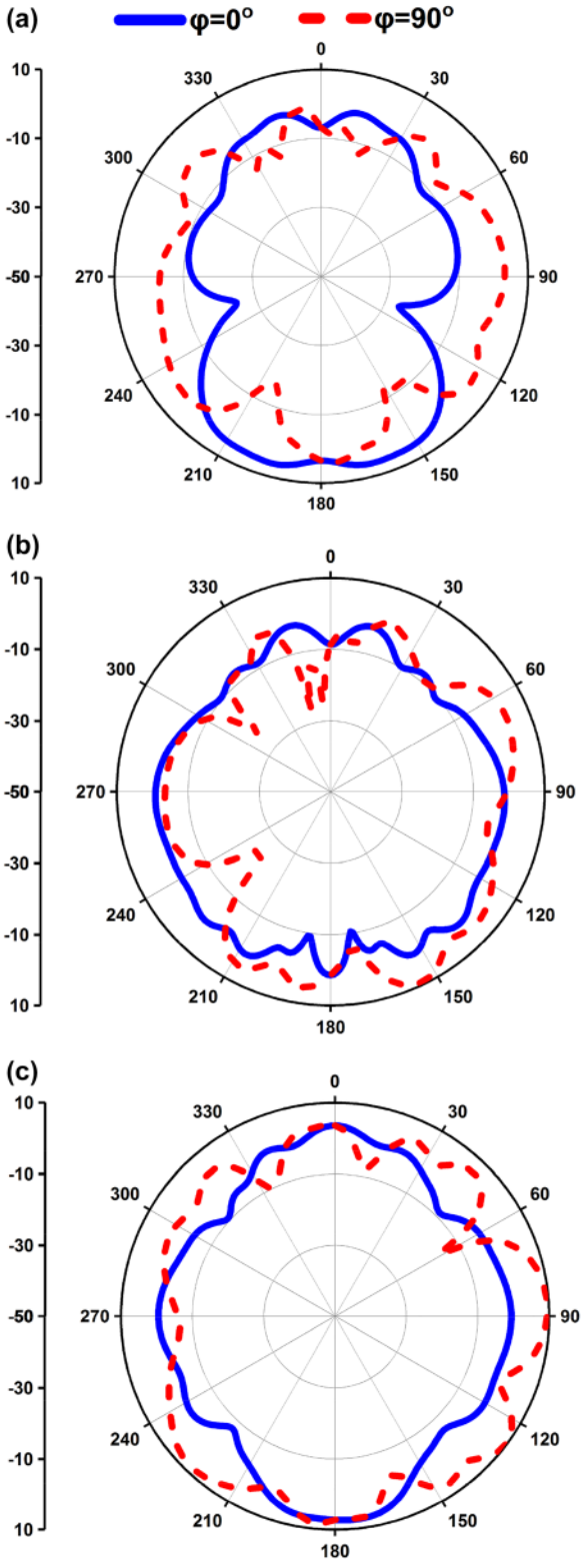

Figure 8: 2D radiation patterns of the proposed graphene antenna array at resonant frequencies: (a) 1.19 THz, (b) 1.297 THz and (c) 1.379 THz.

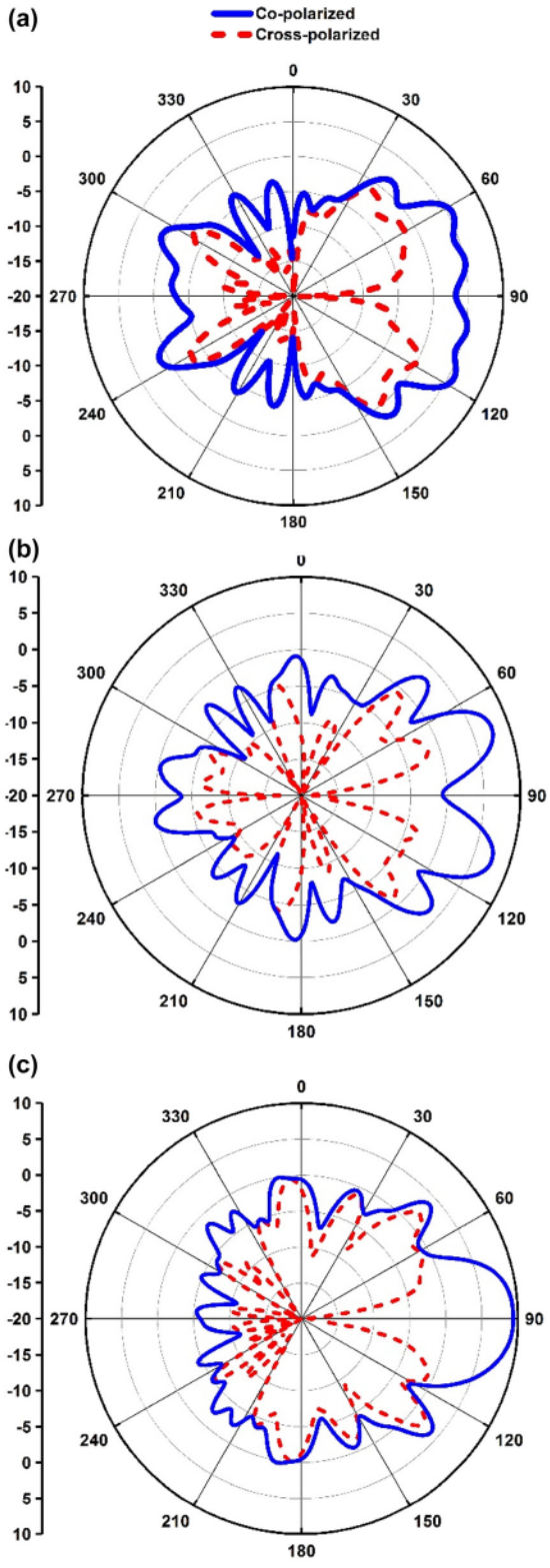

Figure 9: Co and cross polarized components of the proposed graphene antenna array at resonant frequencies: (a) 1.19 THz, (b) 1.297 THz and (c) 1.379 THz.

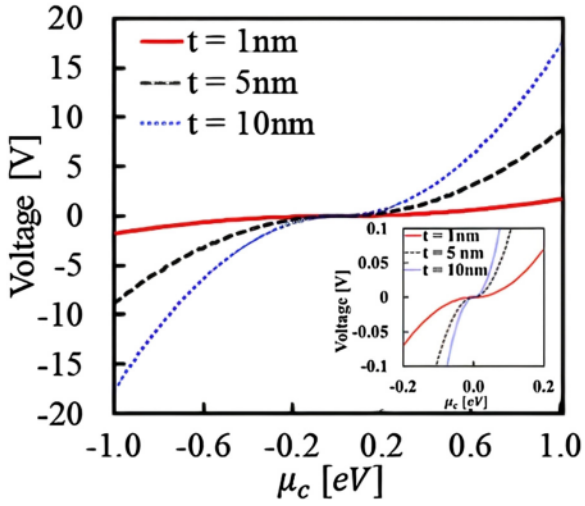

Figure 10: The relation the chemical potential μ_c and the applied bias for different graphene patch thickness [27].

3.5 Comparison with recent works

Table 4 compares the performance characteristics of the proposed antenna array to those of other previously reported THz antennas.

4 Conclusions

In this paper, one simple configuration is used to obtain triple-band in a graphene-based antenna array. The FDTD based CST software is engaged in simulating the antenna array structure to obtain the S-parameter, gain, radiation efficiency, surface current densities, and 2D radiation pattern. The effect of different chemical potentials on the performance of the antenna array is then studied to show how they affect this antenna. It is observed that the performance of the antenna array when applying external voltage indicates good improvements in terms of gain and radiation efficiency. The array's gain and efficiency witness an improvement by 1.3 dB and 10% for μ_c = 0.12 eV, respectively, compared to μ_c = 0 eV. The comparison reveals that the suggested antenna array has better gain and radiation efficiency to the references mentioned, indicating that the proposed design is successful. It is simpler and less expensive to adopt and implement in practice for large scale manufacturing, making it a potential choice for terahertz wireless applications.

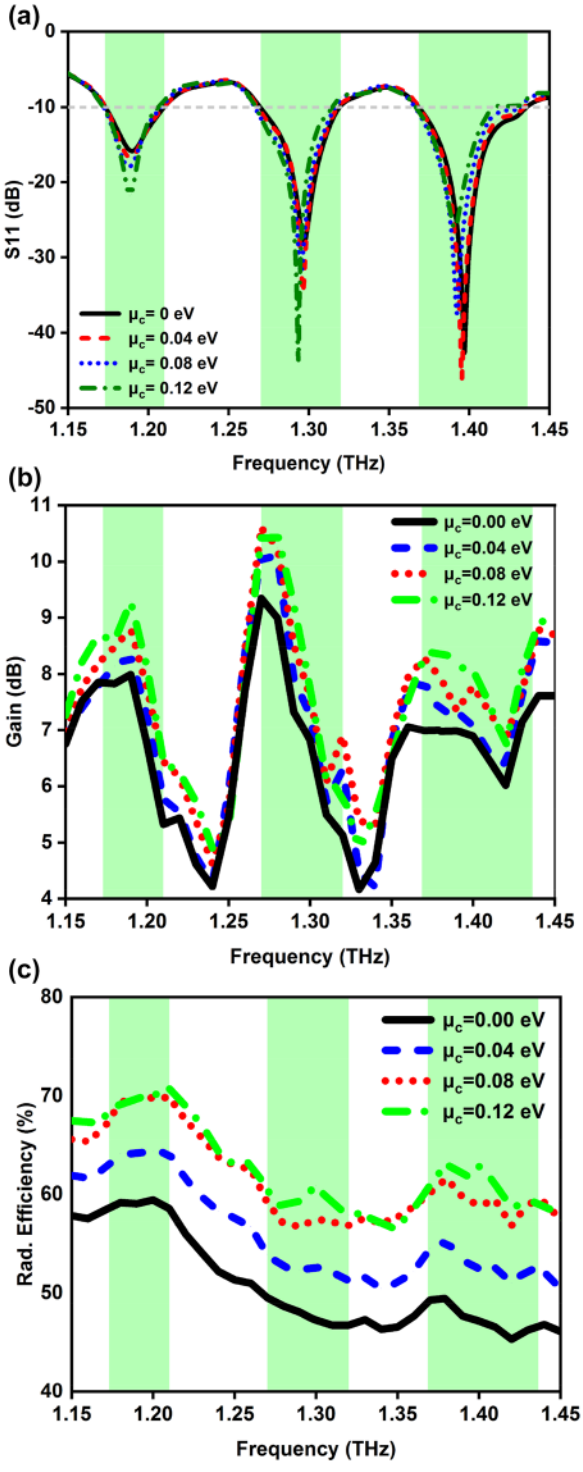

Figure 11: Antenna array's performance parameters: (a) S11 parameter, (b) gain, and (c) radiation efficiency with the variation in μ_c.

Table 3: Comparison of the array performance for different values of the chemical potential μ_c.

Chemical potential μ_c (eV)	Resonant frequencies (THz)	Maximum realized gain (dB)	Maximum radiation efficiency (%)
0.00	1.19, 1.297, 1.397	9.34	59.46
0.04	1.189, 1.2965, 1.3955	10.09	64.13
0.08	1.188, 1.295, 1.392	10.60	69.73
0.12	1.1885, 1.2935, 1.391	10.45	70.00

Table 4: State-of-the-art comparison.

References	Type	Size (μm^3)	Operating frequency (THz)	Maximum gain (dB)	Maximum radiation efficiency (%)	Tunability
[28]	Graphene patch antenna	$100 \times 100 \times 3$	2.15–2.2 and 2.56–2.6	5.03	67.70	Yes
[29]	Metallic patch antenna with PBG substrate	$800 \times 600 \times 191.29$	0.6308–0.6670	7.94	85.71	NA
[30]	Graphene patch antenna	$400 \times 460 \times 100$	0.42–0.48	0.13	24	NA
[31]	Graphene nanoribbon antenna	$770 \times 660 \times 20$	0.630–0.660	9.45	90.60	NA
This work	Graphene patch antenna array	$1000 \times 1000 \times 20$	1.173–1.210, 1.270–1.320 and 1.368–1.346	10.45	70.00	Yes

Author contributions: All the authors have accepted responsibility for the entire content of this submitted manuscript and approved submission.

Research funding: This project has received funding from the Universidad Carlos III de Madrid and the European Union's Horizon 2020 research and innovation program under the Marie Sklodowska-Curie Grant 801538.

Conflict of interest statement: The authors declare that they have no conflicts of interest.

Data availability: All data are included within the manuscript.

References

[1] R. Bala, A. Marwaha, and S. Marwaha, "Graphene antenna design for terahertz regime with exact formulation of surface conductivity," *J. Nanoelectron. Optoelectron.*, vol. 11, no. 4, pp. 459–464, 2016.

[2] K. M. S. Huq, S. A. Busari, J. Rodriguez, V. Frascolla, W. Bazzi, and D. C. Sicker, "Terahertz-enabled wireless system for beyond-5g ultra-fast networks: a brief survey," *IEEE Netw.*, vol. 33, no. 4, pp. 89–95, 2019.

[3] M. N. E. Temmar, A. Hocini, D. Khedrouche, and T. A. Denidni, "Analysis and design of MIMO indoor communication system using terahertz patch antenna based on photonic crystal with graphene," *Photonics Nanostruct. Fundam. Appl.*, vol. 43, p. 100867, 2021.

[4] J. M. Jornet and I. F. Akyildiz, "Channel modeling and capacity analysis for electromagnetic wireless nanonetworks in the terahertz band," *IEEE Trans. Wireless Commun.*, vol. 10, no. 10, pp. 3211–3221, 2011.

[5] L. P. Shi, Q. H. Zhang, S. H. Zhang, C. Yi, and G. X. Liu, "Efficient graphene reconfigurable reflectarray antenna electromagnetic response prediction using deep learning," *IEEE Access*, vol. 9, pp. 22671–22678, 2021.

[6] J. Perruisseau-Carrier, "Graphene for antenna applications: opportunities and challenges from microwaves to THz," in *2012 Loughborough Antennas & Propagation Conference (LAPC)*, Loughborough, UK, LAPC, 2012, pp. 1–4.

[7] Y. Wu, M. Qu, L. Jiao, Y. Liu, and Z. Ghassemlooy, "Graphene-based Yagi-Uda antenna with reconfigurable radiation patterns," *AIP Adv.*, vol. 6, no. 6, 2016, Art no. 065308.

[8] G. Varshney, "Reconfigurable graphene antenna for THz applications: a mode conversion approach," *Nanotechnology*, vol. 31, no. 13, p. 135208, 2020.

[9] S. A. Naghdehforushha and G. Moradi, "High directivity plasmonic graphene-based patch array antennas with tunable THz band communications," *Optik*, vol. 168, pp. 440–445, 2018.

[10] R. K. Kushwaha and P. Karuppanan, "Parasitic-coupled high-gain graphene antenna employed on PBG dielectric grating substrate for THz applications," *Microw. Opt. Technol. Lett.*, vol. 62, pp. 439–447, 2020.

[11] J. N. George and M. G. Madhan, "Analysis of single band and dual band graphene-based patch antenna for terahertz region," *Phys. E Low-dimens. Syst. Nanostruct.*, vol. 94, pp. 126–131, 2017.

[12] M. Dashti and J. D. Carey, "Graphene microstrip patch Ultrawide band antennas for THz communications," *Adv. Funct. Mater.*, vol. 28, no. 11, p. 1705925, 2018.

[13] S. N. H. Sa'don, M. H. Jamaluddin, M. R. Kamarudin, et al., "Characterisation of tunable graphene antenna," *AEU – Int. J. Electron. Commun.*, vol. 118, p. 153170, 2020.
[14] X. Cheng, Y. Wu, J. Yu, S.-W. Qu, Y. Yao, and X. Chen, "Circular beam-reconfigurable antenna base on graphene-metal hybrid," *Electron. Lett.*, vol. 52, pp. 494–496, 2016.
[15] F. Kazemi, "High Q-factor compact and reconfigurable THz aperture antenna based on graphene loads for detecting breast cancer cells," *Superlattice. Microst.*, vol. 153, p. 106865, 2021.
[16] C. Wang, Y. Yao, J. Yu, and X. Chen, "3d beam reconfigurable THz antenna with graphene-based high-impedance surface," *Electronics*, vol. 8, no. 11, p. 1291, 2019.
[17] R. Bala, A. Marwaha, and S. Marwaha, "Performance enhancement of patch antenna in terahertz region using graphene," *Curr. Nanosci.*, vol. 12, no. 2, pp. 237–243, 2016.
[18] R. K. Kushwaha and P. Karuppanan, "Proximity-coupled high gain graphene patch antenna using holey dielectric superstrate for terahertz applications," *Optik*, vol. 240, p. 166793, 2021.
[19] V. Dmitriev, N. R. N. M. Rodrigues, R. M. S. de Oliveira, and R. R. Paiva, "Graphene rectangular loop antenna for terahertz communications," *IEEE Trans. Antenn. Propag.*, vol. 69, no. 6, pp. 3063–3073, 2021.
[20] G. Varshney, S. Gotra, V. S. Pandey, and R. S. Yaduvanshi, "Proximity-coupled two-port multi-input-multi-output graphene antenna with pattern diversity for THz applications," *Nano Commun. Netw.*, vol. 21, p. 100246, 2019.
[21] Y. Luo, Q. Zeng, X. Yan, et al., "Graphene-based multi-beam reconfigurable THz antennas," *IEEE Access*, vol. 7, pp. 30802–30808, 2019.
[22] I. Llatser, C. Kremers, A. Cabellos-Aparicio, J. M. Jornet, E. Alarcón, and N. D. Chigrin, "Graphene-based nano-patch antenna for terahertz radiation," *Photonics Nanostruct. Fundam. Appl.*, vol. 10, no. 4, pp. 353–358, 2012.
[23] M. Y. Han, B. Oezyilmaz, Y. Zhang, and P. Kim, "Energy band gap engineering of graphene nanoribbons," *Phys. Rev. Lett.*, vol. 98, p. 206805, 2007.
[24] G. W. Hanson, "Dyadic Green's functions for an anisotropic, non-local model of biased graphene," *IEEE Trans. Antenn. Propag.*, vol. 56, no. 3, pp. 747–757, 2008.
[25] G. Varshney, A. Verma, V. S. Pandey, R. S. Yaduvanshi, and R. Bala, "A proximity coupleld wideband graphene antenna with the generation of higher order TM modes for THz applications," *Opt. Mater. (Amst)*, vol. 85, pp. 456–463, 2018.
[26] C. H. Gan, H. S. Chu, and E. P. Li, "Synthesis of highly confined surface plasmon modes with doped graphene sheets in the mid-infrared and terahertz frequencies," *Phys. Rev. B*, vol. 85, p. 125431, 2012.
[27] G. Varshney, A. Verma, V. Pandey, R. S. Yaduvanshi, and R. Bala, "A proximity coupled wideband graphene antenna with the generation of higher order TM modes for THz applications," *Opt. Mater.*, vol. 85, pp. 456–463, 2018.
[28] S. Mrunalini and A. Manoharan, "Dual-band reconfigurable graphene-based patch antenna in terahertz band for wireless network-on-chip applications," *IET Microw, Antennas Propag.*, vol. 11, no. 14, pp. 2104–2108, 2017.
[29] R. K. Kushwaha, P. Karuppanan, and L. Malviya, "Design and analysis of novel microstrip patch antenna on photonic crystal in THz," *Phys. B Condens. Matter*, vol. 545, pp. 107–112, 2018.
[30] M. J. Chashmi, P. Rezaei, and N. Kiani, "Y-shaped graphenebased antenna with switchable circular polarization," *Optik (Stuttg)*, vol. 200, p. 163321, 2019.
[31] I. Ahmad, S. Ullah, S. Ullah, et al., "Design and analysis of a photonic crystal based planar antenna for THz applications," *Electronics*, vol. 10, p. 1941, 2021.